

Bistable analytic-phase synchronization in strongly competing chaotic lasing modes.

Sebastian Wieczorek and Weng W. Chow
Sandia National Laboratories, Albuquerque NM 87185/0601, USA
 (November 10, 2018)

We theoretically study analytic-phase synchronization in strongly-competing oscillator systems. Using the example of composite-cavity modes coupled via a class-B laser active medium, we discover that inherent chaotic phase synchronization can arise concurrently at two different chaotic attractors, leading to bistable phase-synchronized solutions. In our example, the underlying mechanism for bistability and inherent phase synchronization is population pulsation within the active medium.

PACS numbers: 05.45.Xt, 42.60.Mi, 42.65.Sf, 42.55.Px,

Synchronization of interacting oscillators is encountered in many physical, chemical, and biological systems. Recently, considerable research has been devoted to understanding why and under what conditions chaotic synchronization is possible [1]. In chaotic synchronization, two (or more) chaotic oscillators adjust a given property of their motion to a common behavior, as a result of coupling. Depending on the property under consideration, different types of chaotic synchronization were recognized; see [1] and references therein. Chaotic phase synchronization, which is the subject of this paper, occurs when the phase difference of interacting chaotic oscillators remains bounded within the range of 2π for all time (phase locking) [2].

There are different approaches to achieving chaotic synchronization. A typical setup involves initially independent oscillators, where at least one is chaotic. Then, these oscillators (e.g. chaotic lasers) are made to interact with each other, and the focus of existing studies is on either an unidirectional or a bidirectional coupling scheme [1–9]. Another approach uses external modulation of a system of interacting oscillators to force chaotic synchronization, e.g. as in an experiment involving a modulated three-mode solid state laser [10]. Less understood and perhaps most interesting is inherent chaotic synchronization where the chaos and chaotic synchronization arise entirely from instabilities induced by the mutual coupling between the oscillators, without requiring chaos in uncoupled oscillators. Inherent chaotic synchronization was detected experimentally and studied numerically for lasers coupled at a distance [11–14]. However, the underlying physical mechanism remains unclear. Moreover, in all these studies, the chaotic-synchronized oscillators appear to involve a single chaotic attractor [1–14].

This paper investigates inherent chaotic phase synchronization within the scope of strongly-competing oscillators. Considering two composite-cavity modes coupled via class-B active medium [15] we are able to definitely identify the physical mechanism enabling phase synchronization to be an intrinsic behavior of this system. Furthermore, we discovered that the chaotic phase synchronization in strongly-competing oscillators exhibits bistability, a phenomenon that has not been reported previously. Also, we found that, in contrast to chaotic phase synchronization of oscillators that are independently chaotic, transition to inherent chaotic phase synchronization is not clear-cut.

We consider a double-cavity laser, where cavity A of length L is coupled via a common mirror of transmission T to cavity B of length $L + dL$. There are two approaches to model such a system [15]. (i) In the more phenomenological one, lasers are treated as individual oscillators and the coupling is introduced via *ad hoc* terms in the equations of motion for uncoupled lasers. (ii) In an alternate approach, called composite-cavity mode approach, the entire coupled-laser structure is treated as a single system. The lasing field is decomposed in terms of the eigenmodes extending over both cavities rather than the fields of individual cavities. In this picture, composite-cavity modes (CCMs), rather than individual lasers, are the interacting oscillators. The slowly varying dimensionless electric field amplitudes E_n , and optical phases ψ_n associated with the n -th CCM evolve accordingly to [15,17]

$$\dot{E}_n = -\gamma E_n + C_{nn} \gamma \times \sum_k [C_{kn}^A (1 + \beta N^A) + C_{kn}^B (1 + \beta N^B)] \cos(\psi_{kn}) E_k, \quad (1)$$

$$\dot{\psi}_n = \Omega_n + C_{nn} \gamma \times \sum_k [C_{kn}^A (1 + \beta N^A) + C_{kn}^B (1 + \beta N^B)] \sin(\psi_{kn}) \frac{E_k}{E_n}, \quad (2)$$

where γ is the ratio between photon and population decay rates, β is the dimensionless gain coefficient, Ω_n is the dimensionless passive CCM frequency, and $\psi_{kn} = \psi_k - \psi_n$ [17]. In class-B lasers, the active-medium polarization decays much faster than the population and electric field. Then, the evolution of the dimensionless population N is governed by [17]

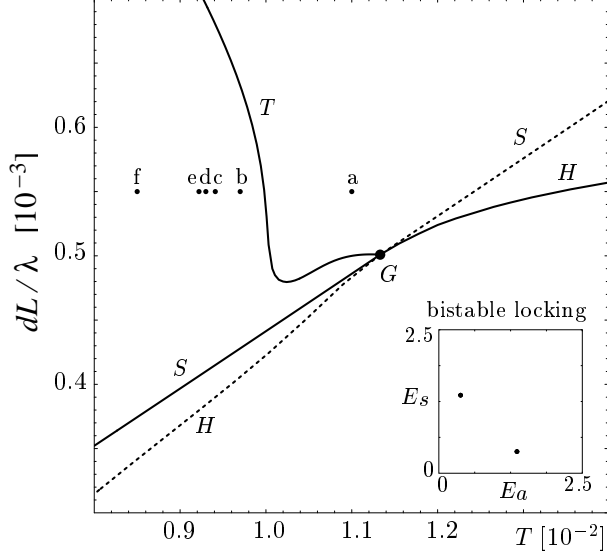


FIG. 1. Bifurcation diagram near saddle-node-Hopf point G . Inset shows bistability inside the locking region. The dots a-f denote parameters for the panels in Fig. 2.

$$\dot{N}_{A(B)} = \Lambda_{A(B)} - (N_{A(B)} + 1) + - \sum_{m,n} C_{nm}^{A(B)} (1 + \beta N^{A(B)}) \cos(\psi_{nm}) E_m E_n, \quad (3)$$

where $\Lambda_{A(B)}$ is the dimensionless excitation rate in cavity $A(B)$. The T and dL dependent $C_{nn}^{A(B)}$ describes the overlap of the n -th CCM with the active gain medium in cavity $A(B)$, and the nonlinearities due to optical coupling between the cavities [17]. We consider two CCMs, called symmetric ($n = s$) and antisymmetric ($n = a$) to refer to the relative optical phases between the fields in individual resonators [16]. For the calculations we use $\gamma = 2 \times 10^{11} \text{ s}^{-1} / (2 \times 10^9 \text{ s}^{-1}) = 100$, $\beta = 5.41$, $\Lambda = 2$, and $L = 280 \mu\text{m}$ [17].

The two sources of coupling (cross-saturation) between CCMs u_n are spatial and spectral hole burning. In spatial hole burning, proportional to

$$\mathcal{C}_{nm} = \sum_{i=A,B} C_{nn}^i C_{mm}^i = \frac{1}{L} \left[\int_{-L}^0 dz u_n^2(z, T, L, dL) \int_{-L}^0 dz' u_m^2(z', T, L, dL) + \int_0^{L+dL} dz u_n^2(z, T, L, dL) \int_0^{L+dL} dz' u_m^2(z', T, L, dL) \right], \quad (4)$$

competition arises because both CCMs deplete population at the same locations in the active medium [15]. In spectral hole burning, the electric field of one CCM saturates population at the frequency of the other CCM. One contribution to spectral hole burning comes from population pulsation, a result of nonlinear composite-mode interaction where the active-medium population acquires an oscillation at the intermode frequency [$n \neq m$ terms in Eq. (3)]. This oscillation interacts with the n -th CCM to modify the active-medium polarization at the frequency of the m -th CCM. Consequently, more competition arises due to additional cross-saturation of the m -th CCM. Under appropriate conditions, the additional cross-saturation leads to strong competition resulting in bistability between stable stationary points [16,17].

Coupling between CCMs is adjusted with T and dL . For $T = 0$ and $dL \neq 0$, $\mathcal{C}_{sa} = 0$ and the two CCMs are uncoupled: each CCM becomes a mode of a different individual laser [16]. Recall, that we study inherent chaotic synchronization and the two CCMs are not chaotic at zero coupling. For $|dL| > 0$, coupling increases with T [17]. As a result, the two interacting CCMs turn chaotic and exhibit transition to chaotic phase synchronization.

Applying bifurcation continuation techniques [18] to Eqs. (1-3), we calculated saddle-node S , Hopf H , and torus T bifurcation curves in the parameter space $(T, dL/\lambda)$ [Fig. 1]. Curves S and H are tangent at saddle-node-Hopf points G where they change their type. Supercritical bifurcations of attractors are plotted as solid curves and subcritical bifurcations of unstable objects are plotted as dashed curves. Inside the lockband, which extends below the solid parts of S and H , composite modes are phase locked to operate at constant intensity and the same optical frequency. Moreover, there exist two stable stationary points in the $\{E_a, E_s, \psi_{sa}, N_A, N_B\}$ phase space. Depending on initial conditions, the system of coupled CCMs settles through strong competition to oscillate at an optical frequency that is

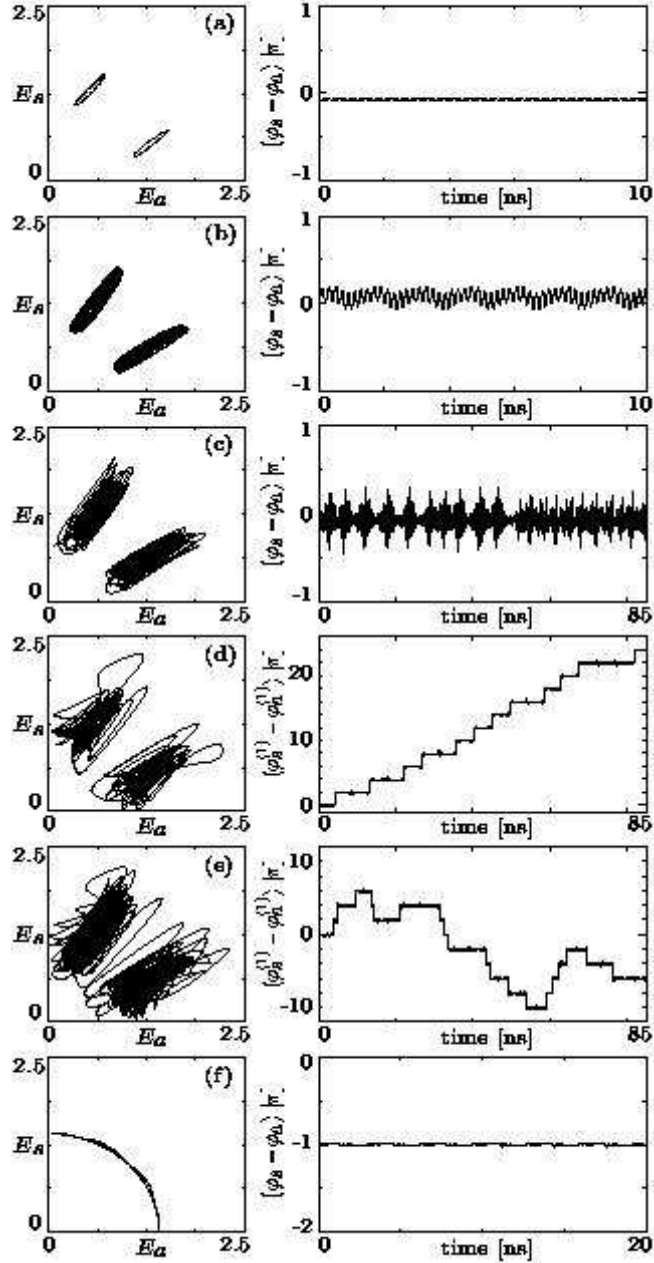


FIG. 2. (first column) Phase portraits and (second column) time evolution of the analytic-phase difference for the transition at $dL/\lambda = 0.55 \times 10^{-3}$. From (a) to (f) $T [10^{-2}] = 1.1, 0.97, 0.94, 0.93, 0.924$, and 0.85 . Refer to the dots a-f in Fig. 1. The time evolution of the analytic-phase difference is shown for the lower of the two coexisting attractors.

near the frequency of either symmetric or antisymmetric CCM. Each bifurcation curve in Fig. 1 denotes bifurcations of the two attractors [17].

Outside the lockband, optical-phase locking to a single optical frequency is lost and the modal intensities oscillate. Even when they are irregular, these oscillations may still exhibit certain types of synchronization when described with appropriate variables. Here, the appropriate quantity is the analytic phase φ_k of a real signal $x_k(t) = E_k^2(t) - \langle E_k^2(t) \rangle$, that is defined through $x_k(t) + i\tilde{x}_k(t) = \sqrt{x_k^2(t) + \tilde{x}_k^2(t)} \exp[i\varphi_k(t)]$, where $\langle E_k^2(t) \rangle = \lim_{T \rightarrow \infty} \int_0^T [E_k^2(t)/T] dt$, \tilde{x}_k is the Hilbert transform of x_k [19], and $k = a, s$. Analytic phase φ_k is well defined if the trajectory in the complex plane (x_k, \tilde{x}_k) has one center of rotation. In the case of multiple centers of rotation, the signal needs to be decomposed

into

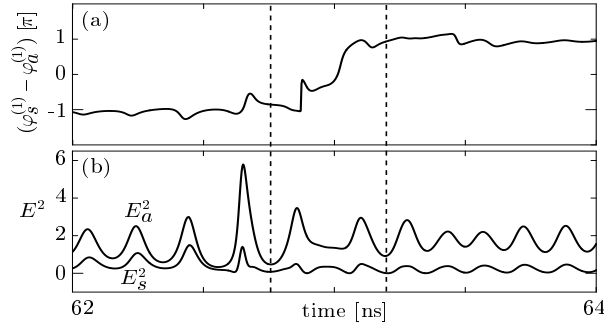


FIG. 3. (a) An example of a 2π jump in the analytic-phase difference [compare with Fig. 2 (d)] and (b) the corresponding chaotic oscillations of the coupled composite-cavity modes.

intrinsic modes $x_k(t) = \sum_j x_k^{(j)}(t)$ such that the trajectory in the plane $(x_k^{(j)}, \tilde{x}_k^{(j)})$ has one center of rotation [20]. In this paper, we use $\varphi_k^{(1)}$ whenever chaotic attractor has multiple centers of rotation. The analytic phase φ_k of the modal intensity is distinctly different from the optical phase ψ_k .

When the solid part of H is crossed from below to above in Fig. 1, locking of optical phases is lost. Each of the two coexisting stationary points turns unstable and gives rise to a stable periodic orbit. The relaxation oscillation, which is a characteristic of a class-B laser, become undamped. Now, both CCMs selfpulsate but their analytic phases are locked [Fig. 2 (a)]. Periodic oscillation can undergo further instabilities. Torus bifurcation curve T emerging from G marks the transition to quasiperiodic oscillation that involves two frequencies: the relaxation oscillation frequency and the CCM beatnote. Dynamics on the two tori also show analytic-phase synchronization [Fig. 2 (b)]. Decreasing T further leads to the break-up of coexisting tori into chaotic attractors. Despite chaotic oscillations in both CCMs, their analytic-phase difference remains within a range of 2π for all time [Fig. 2 (c)]. Inherent chaotic phase synchronization is present simultaneously at two different chaotic attractors. Upon further decrease in the coupling, analytic-phase synchronization is lost [Fig. 2 (d)]. The analytic-phase difference for the lower (upper) chaotic attractor increases (decreases) in time exhibiting 2π jumps (Fig. 3). Next, the two chaotic attractors merge into one chaotic attractor [Fig. 2 (e)]. The analytic phases remain unlocked but the direction of 2π jumps alternates as a result of transitions between the two formerly bistable chaotic attractors.

To see how the changes in analytic-phase synchronization of coupled chaotic CCMs come about, we plot in Fig. 4 the maxima of E_a^2 versus T . The simulation starts at higher T with two chaotic attractors, the lower and the upper. As T decreases, changes in the chaotic dynamics appear, including windows of periodicity called Arnold tongues. We find that analytic-phase synchronization is lost after transition through an Arnold tongue. At the right hand side of the widest Arnold tongue in Fig. 4(b), periodic orbit of high period is born and replaces the chaotic attractor. After some bifurcations, this orbit disappears to give place to a new chaotic attractor. However, the chaotic attractor that appears at the left hand side of this Arnold tongue [Fig. 5(a)] is significantly different from the chaotic attractor that disappears at the right hand side of this Arnold tongue [Fig. 5(b)]. The change(s) in the structure of the chaotic attractor (possibly due to homoclinic or heteroclinic tangency between stable and unstable manifolds of some saddle orbits) result in phase desynchronization. Analytic-phase difference for chaotic attractor at the left hand side of the Arnold tongue shows 2π phase jumps that become more frequent with decreasing T [Fig. 5(c)]. Similar changes take place in the upper chaotic attractor. Although the detailed bifurcation scenario inside the (narrow) Arnold tongue in Fig. 4(a) is different, the resulting effect is the same: phase-desynchronized chaotic attractor emerges. It is important to note that within desynchronized chaos we find Arnold tongues with dynamics that still show analytic-phase synchronization [arrow at the bottom of Fig 4(a)]. Therefore, transition to chaotic phase synchronization of independently stable oscillators is not as clear-cut as for oscillators that are independently chaotic [2].

As T decreases further, the lower chaotic attractor hits the basin boundary that separates the two chaotic attractors, and is destroyed [right arrow at the bottom of Fig 4(b)]. The trajectory settles to the upper chaotic attractor which then expands onto the remnants of the lower chaotic attractors [middle arrow at the bottom of Fig 4 (b)]. These two crises lead to a single chaotic attractor which is composed of the two formerly bistable attractors. Eventually, the chaotic attractor from Fig. 2 (e) hits the boundary that separates it from a periodic orbit [left arrow at the bottom of Fig 4(b)] and the trajectory settles to the periodic orbit with anti-phase dynamics [Fig. 2 (f)]. This orbit originates at the solid part of S and has a different origin than the periodic orbits in Fig. 2 (a). It arises due to unlocking of optical phases of the two CCMs [15,17]. Upon increasing T , this anti-phase oscillation coexists with in-phase oscillations, until it disappears in a saddle-node-of-periodic-orbit bifurcation at $T \sim 1.1 \times 10^{-2}$.

Different physical mechanisms are responsible for in-phase and out-of-phase synchronization. On the one hand,

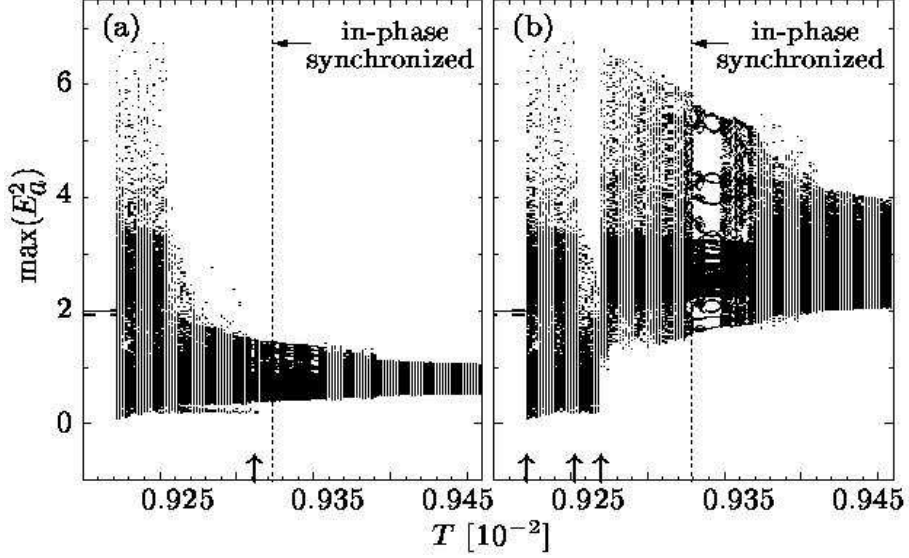


FIG. 4. Bifurcations of the (a) upper and (b) lower chaotic attractor with decreasing T , leading to a loss of phase synchronization and subsequently to a single chaotic attractor.

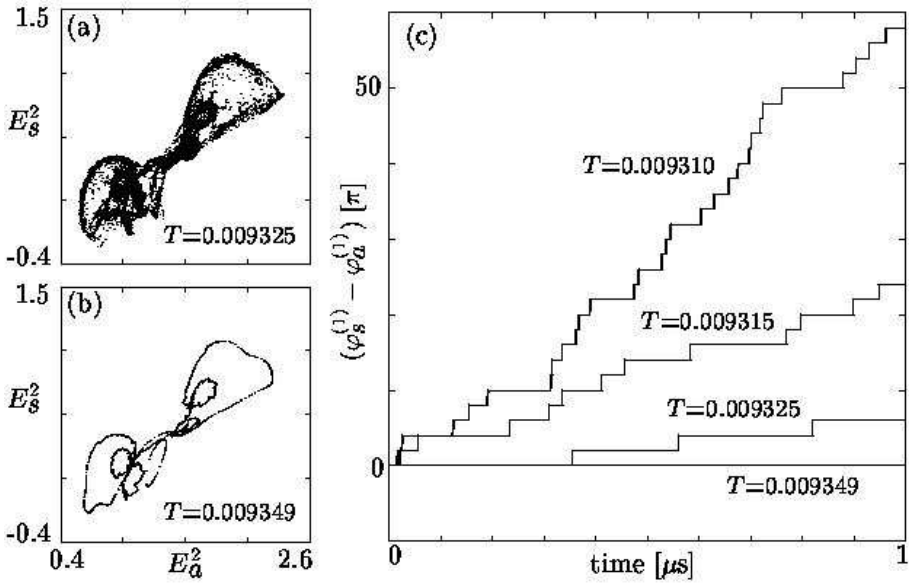


FIG. 5. (a-b) Change in the internal structure of the lower chaotic attractor due to transition through an Arnold tongue shown as a Poincaré section defined by $\{N_A = 0.025\}$ [compare with Fig. 4(b)], and (c) the resulting loss of chaotic phase synchronization.

when composite-mode detuning is too large for the optical phases to lock, but close to the relaxation oscillation frequency ($T \gtrsim 1.1 \times 10^{-2}$ and outside lockband), population pulsation provides an inherent source of modulation that can excite self-sustained relaxation oscillation and force in-phase dynamics of modal intensities. On the other hand, when CCM frequencies are close enough ($T \lesssim 1.1 \times 10^{-2}$ and outside lockband) the optical-phase locking terms become significant. Then, the system of two coupled CCMs alternates between the two states of nearly single-CCM operation, resulting in anti-phase dynamics. For intermediate conditions, in-phase and anti-phase dynamics can

coexist. Strong population pulsation effects are crucial for the inherent chaotic phase synchronization to occur. If they are neglected, neither bistability nor the instabilities leading to synchronization are present.

In conclusion, we extended the usual analysis of chaotic phase synchronization to strongly-competing oscillators, where system dynamics are more diversified and less understood. In addition to previously reported results, the present analysis shows that chaotic phase synchronization can occur in coupled oscillators that are independently stable. This inherent chaotic phase synchronization results solely from the nonlinearities associated with strong mode competition within a saturable active medium. In the presence of population pulsation, strong competition causes the phenomenon to appear simultaneously at two different chaotic attractors, giving rise to bistable chaotic-phase-synchronized solutions. In contrast to phase synchronization of independently chaotic oscillators, transition to (inherent) phase synchronization of independently stable oscillators is not clear-cut: windows of phase-synchronized dynamics are found within phase-desynchronized chaos.

This work is partially funded by the US Department of Energy under contract DE-AC04-94AL8500. WC acknowledges support from the Research Award of the Alexander von Humboldt Foundation.

-
- [1] S. Boccaletti et al., *Phys. Rep.* **366** (2002) 1.
 - [2] M.G. Rosenblum, A.S. Pikovsky, and J. Kürths, *Phys. Rev. Lett.* **76** (1996) 1804.
 - [3] S. Boccaletti et al., *Phys. Rev. Lett.* **89** (2002) 194101.
 - [4] R. Breban and E. Ott, *Phys. Rev. E* **65** (2002) 056219.
 - [5] R. McAllister et al., *Phys. Rev. E* **67** (2003) 015202(R).
 - [6] G.V. Osipov et al., *Phys. Rev. Lett.* **91** (2003) 024101.
 - [7] R. Roy and K.S. Thornburg Jr., *Phys. Rev. Lett.* **72** (1994) 2009.
 - [8] M. Peil, et al. *Phys. Rev. Lett.* **88** (2002) 174101.
 - [9] I. Leyva et al., *Phys. Rev. E* **68** (2003) 066209.
 - [10] K. Otsuka et al., *Chaos* **12** (2002) 678.
 - [11] T. Heil, I. Fischer, and W. Elsäßer, *Phys. Rev. Lett.* **86** (2001) 795.
 - [12] D.J. DeShazer et al., *Phys. Rev. Lett.* **87** (2001) 044101.
 - [13] C.R. Mirasso et al., *Phys. Rev. A* **65** (2001) 013805.
 - [14] J. Mulet et al., *J. Opt. B: Quant. Semiclass. Opt.* **6** (2004) 97.
 - [15] S. Wieczorek and W.W. Chow, *Phys. Rev. A* **69** (2004) 033811.
 - [16] W.W. Chow, *IEEE Jour. of Quant. Electron.* **QE-22** (1986) 1174.
 - [17] S. Wieczorek and W.W. Chow, *Opt. Comm.*, to appear.
 - [18] E. Doedel et al., <http://sourceforge.net/projects/auto2000/>.
 - [19] D. Gabor, J. IEEE (London) **93** (1946) 429.
 - [20] T. Yalçinkaya and Y-C. Lai, *Phys. Rev. Lett.* **79** (1997) 3885.